Article

Not peer-reviewed version

Intermittent Hypoxia Induces Cognitive Dysfunction and Hippocampal Gene Expression Changes in a Mouse Model of Obstructive Sleep Apnea

Kenta Miyo , Yuki Uchida * , Ryota Nakano , Shotaro Kamijo , Masahiro Hosonuma , Yoshitaka Yamazaki , Hikaru Isobe , Fumihiro Ishikawa , Hiroshi Onimaru , Akira Yoshikawa , Shin-Ichi Sakakibara , Tatsunori Oguchi , Takuya Yokoe , Masahiko Izumizaki

Posted Date: 27 June 2025

doi: 10.20944/preprints202506.2250.v1

Keywords: obstructive sleep apnea syndrome; intermittent hypoxia; cognitive dysfunction; hippocampus; gene expression

 doi:10.20944/preprints202506.2250.v1

Article

Intermittent Hypoxia Induces Cognitive Dysfunction and Hippocampal Gene Expression Changes in a Mouse Model of Obstructive Sleep Apnea

Kenta Miyo [1,2,†], Yuki Uchida [1,*,†], Ryota Nakano [3], Shotaro Kamijo [3], Masahiro Hosonuma [4], Yoshitaka Yamazaki [5], Hikaru Isobe [4], Fumihiro Ishikawa [6], Hiroshi Onimaru [1], Akira Yoshikawa [7], Shin-Ichi Sakakibara [8], Tatsunori Oguchi [4], Takuya Yokoe [2] and Masahiko Izumizaki [1]

[1] Department of Physiology, Showa Medical University School of Medicine, Tokyo, Japan
[2] Department of Respiratory Medicine, Showa Medical University Fujigaoka Hospital, Yokohama, Japan
[3] Department of Physiology, Showa Medical University Graduate School of Pharmacy, Tokyo, Japan
[4] Division of Medical Pharmacology, Department of Pharmacology, Showa Medical University School of Medicine, Tokyo, Japan
[5] Division of Toxicology, Showa University Graduate School of Pharmacy, Tokyo, Japan
[6] Center for Biotechnology, Showa Medical University, Tokyo, Japan
[7] Division of Health Science Education, Showa Medical University School of Nursing and Rehabilitation Sciences, Yokohama, Japan
[8] Laboratory for Molecular Neurobiology, Faculty of Human Sciences, Waseda University, Tokorozawa, Saitama, Japan
* Correspondence: yukioto@med.showa-u.ac.jp; Tel.: +81-03-3784-8113
† These authors contributed equally to this work.

Abstract: Obstructive sleep apnea syndrome (OSAS) is characterized by cycles of decreased blood oxygen saturation followed by reoxygenation due to transient apnea. Cognitive dysfunction is a complication of OSAS, but its mechanisms remain unclear. 8-week-old C57BL/6J mice were exposed to intermittent hypoxia (IH) to model OSAS, and cognitive function and hippocampal gene expression were analyzed. Three groups were maintained for 28 days: IH group (oxygen alternating between 10–21% in 2-minute cycles, 8 hours/day), sustained hypoxia group (SH) (10% oxygen, 8 hours/day), and control group (21% oxygen). Behavioral tests and RNA sequencing (RNA-seq) analysis was performed. While Y-maze test results showed no differences, the IH group demonstrated impaired memory and learning in passive avoidance tests compared to control and SH groups. RNA-seq revealed specific changes in learning/memory-related genes and oxidative stress response genes in the IH group. RT-qPCR showed decreased *Lars2*, *Hmcn1*, and *Vstm2l* expression in the IH group. Pathway analysis showed the suppression of the KEAP1-NFE2L2 antioxidant pathway in the IH group vs. SH group. Our findings demonstrate that IH may cause cognitive dysfunction through oxidative stress and suppressed antioxidant defenses. IH-specific downregulation of *Lars2*, *Hmcn1*, and *Vstm2l* may contribute to OSAS-related cognitive impairment.

Keywords: obstructive sleep apnea syndrome; intermittent hypoxia; cognitive dysfunction; hippocampus; gene expression

 doi:10.20944/preprints202506.2250.v1

1. Introduction

Obstructive sleep apnea syndrome (OSAS) is the most common sleep-related breathing disorder, with a prevalence of 13–33% in men and 6–19% in women [1], affecting approximately 1 billion people worldwide [2]. The fundamental pathophysiological feature of OSAS is recurrent upper airway obstruction during sleep, leading to cycles of hypoxia followed by reoxygenation [3].

OSAS presents diverse clinical manifestations, including snoring, excessive daytime sleepiness, and choking sensations during sleep. OSAS significantly affects multiple organ systems and increases the risk of hypertension [4], type 2 diabetes [5], and cardiovascular diseases [6]. Among these complications, cognitive dysfunction has emerged as an important complication of OSAS [7]. Patients with OSAS experience impaired attention, memory deficits, learning difficulties, and executive dysfunction [8,9]. Moreover, OSAS has been associated with increased risk of mild cognitive impairment and dementia [10].

The hippocampus plays a central role in memory formation and consolidation. Neuroimaging studies have revealed hippocampal atrophy in OSAS patients, correlating with decreased memory and learning functions [11]. At the cellular level, OSAS impairs synaptic plasticity in the hippocampal CA1 region and reduces neuronal numbers in both CA1 and CA3 regions [12,13]. However, the precise molecular mechanisms underlying OSAS-induced cognitive dysfunction remain poorly understood.

Intermittent hypoxia (IH) is a core pathophysiological condition in OSAS. In mouse IH models, cycling oxygen concentrations are used to reproduce hypoxia-reoxygenation cycles that mimic OSAS. Mice exposed to IH have shown impairments in spatial cognition, working memory, and learning in behavioral tests such as the Morris water maze test [14], Y-maze test [15], and passive avoidance test [16]. These cognitive dysfunctions involve not only decreased oxygen utilization due to hypoxia but also oxidative stress resulting from increased production of reactive oxygen species (ROS) during reoxygenation [17-19].

While IH-induced cognitive dysfunction has been demonstrated, studies that distinguish and evaluate the effects of hypoxia and reoxygenation in IH are limited, and the precise roles of specific genes and molecular pathways that cause cognitive dysfunction in the hippocampus remain unclear. In this study, we compared IH and sustained hypoxia (SH) groups to investigate the differential effects of reoxygenation on cognitive function and hippocampal gene expression, aiming to elucidate the molecular mechanisms underlying OSAS-related cognitive dysfunction.

2. Results

2.1. Y-maze Test and Passive Avoidance Test

Figure 1A shows the alternation rate in the Y-maze test. One-way analysis of variance showed no statistically significant effect of exposure conditions ($F(2,46) = 1.460$, $P = 0.243$). Figure 1B shows the proportion of mice that reached 300 seconds without entering the dark side of the chamber on day 2 of the passive avoidance test. A chi-square test among the three groups revealed statistically significant differences between groups ($\chi^2(2) = 10.719$, $P = 0.005$). Pairwise comparisons using chi-square tests with Bonferroni correction showed that the IH group had a significantly lower proportion of mice reaching 300 seconds compared to both the control group ($\chi^2(1) = 8.760$, corrected $P = 0.009$) and the SH group ($\chi^2(1) = 8.429$, corrected $P = 0.011$). No significant difference was observed between the control and SH groups ($\chi^2(1) = 0.139$, $P = 0.710$).

 doi:10.20944/preprints202506.2250.v1

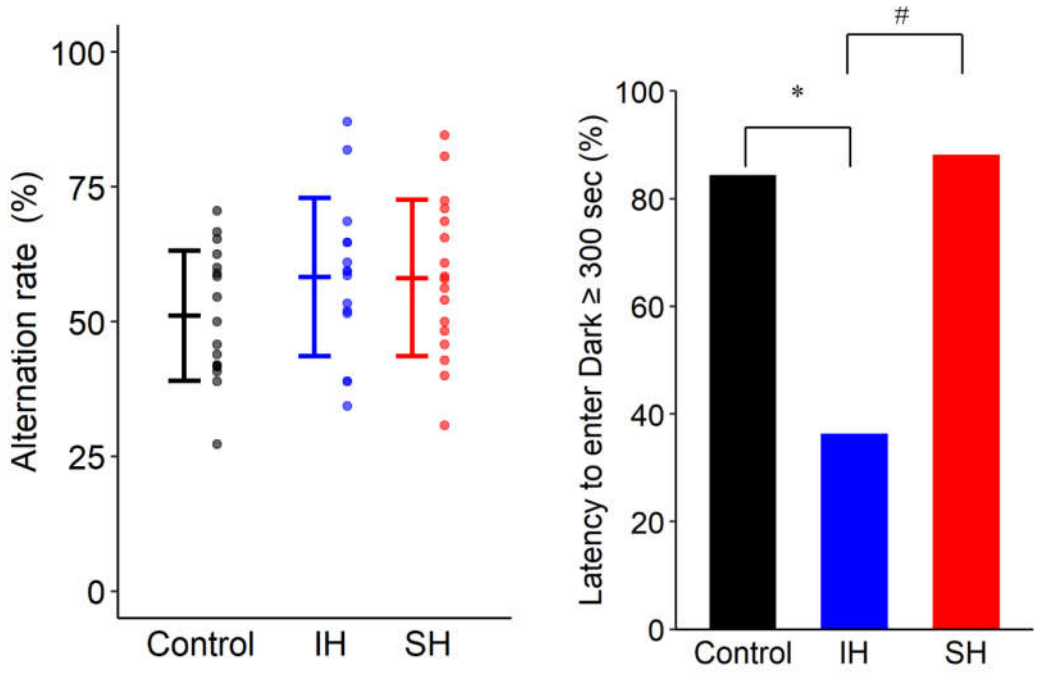

(A) (B)

Figure 1. Behavioral test results. (A) Alternation rate in the Y-maze test. No statistically significant differences were observed among the control, IH, and SH groups ($F(2,46) = 1.460$, $P = 0.243$). (B) Percentage of mice with dark chamber entry latency ≥ 300 seconds in the passive avoidance test. The IH group showed a significantly lower percentage compared to the control group (* $P = 0.009$, Bonferroni-corrected). The IH group also showed a significantly lower percentage compared to the SH group (# $P = 0.011$, Bonferroni-corrected). No significant difference was observed between the control and SH groups ($\chi^2(1) = 0.139$, $P = 0.710$). Data are presented as mean ± standard error (A; Control: n = 17, IH: n = 15, SH: n = 17) or as percentage (B; Control: n = 38, IH: n = 16, SH: n = 17). Statistical significance was set at $P < 0.05$. * $P < 0.05$, IH vs. control; # $P < 0.05$, IH vs. SH. IH, intermittent hypoxia; SH, sustained hypoxia.

2.2. Comparisons of differentially expressed genes (DEGs)

To investigate the effects of IH and SH on gene expression in the mouse hippocampus, RNA sequencing (RNA-seq) was performed. Volcano plots of DEGs are shown in Figure 2A-C. Compared to the control group, the IH group showed 170 downregulated and 46 upregulated genes, while the SH group showed 151 downregulated and 44 upregulated genes. Direct comparison between IH and SH groups revealed 37 downregulated and 19 upregulated genes in the IH group relative to the SH group. The top 50 DEGs in each comparison, ranked by absolute $\log_2$ fold change (FC) magnitude, are shown in Tables 2A, B, and C.

Figure 2D shows a Venn diagram of the DEGs. Venn diagram analysis revealed that 73 genes were shared between IH/control and SH/control comparisons, including *Pknox1* and *Klf2*. Sixteen genes were shared between IH/control and IH/SH comparisons, including *Adrb1*. Twelve genes were shared between IH/SH and SH/control comparisons, including *Dbi*. Two genes (*Cebpb* and *Gng13*) were common to all three comparisons.

 doi:10.20944/preprints202506.2250.v1

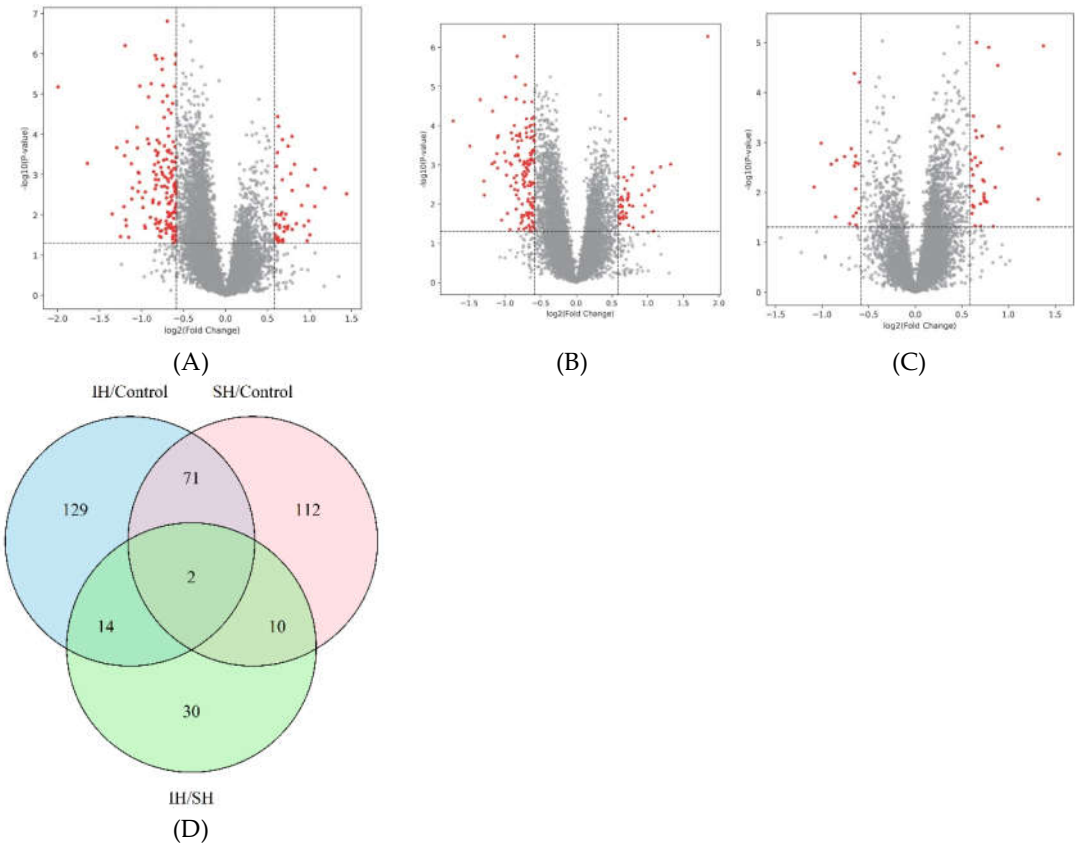

Figure 2. Differentially expressed genes (DEGs) analysis (Control: n = 4, IH and SH: n = 5 each). (A, B, C) Volcano plots showing gene expression changes between different oxygen exposure conditions. (A) IH vs. control, (B) SH vs. control, (C) IH vs. SH. The X-axis shows $\log_2$ fold change (FC); the Y-axis shows $-\log_{10}$ (P-value). Red dots represent DEGs. Statistical significance was set at $|\log_2(FC)| > 0.58$ and $-\log_{10}(P) > 1.3$. (D) Venn diagram of DEGs among the three comparisons. Seventy-three genes were shared between IH vs. control and SH vs. control comparisons, sixteen genes between IH vs. control and IH vs. SH comparisons, and twelve genes between IH vs. SH and SH vs. control comparisons. Two genes were common to all three comparisons. IH, intermittent hypoxia; SH, sustained hypoxia.

Table 1. Probes used for RT-qPCR analysis

Gene	Forward Primer	Reverse Primer	Probe Sequence
Adrb1	5'-GTTTACTCAAGACCGAAAGCAG-3'	5'-CACTCTCCCAACTCCTCCTAA-3'	5'-/56-FAM/ATGCAAAGC/ZEN/CCACAGATCTATCGAATCA/3IABkFQ/-3'
Basp1	5'-CCTTTGCTGAGCGACCA-3'	5'-AGCTTGCCTCCCATCTTG-3'	5'-/56-FAM/TGAGCGCGG/ZEN/TGCCTCCAA/3IABkFQ/-3'
Cebpb	5'-GTTTCGGGACTTGATGCAATC-3'	5'-CCGCAGGAACATCTTTAAGTGA-3'	5'-/56-FAM/ACACGGGAC/ZEN/TGACGCAACACA/3IABkFQ/-3'
Dbi	5'-CATCTACAGTCACTTCAAACAAGC-3'	5'-ACATAGGTCTTCATGGCACTT-3'	5'-/56-FAM/ACTCGTGGA/ZEN/ACAAGCTGAAAGGAC/3IABkFQ/-3'

 doi:10.20944/preprints202506.2250.v1

	5'-AGGATAAAGCGACAGCAAC-3'	5'-CACCATGAACTCTTGCCAGT-3'	5'-/56-FAM/AGAACTCCA/ZEN/TTCGGCACAACCTGT/3IABkFQ/-3'
Foxo6			
	5'-CAGGAAGGTGGCATGGTT-3'	5'-TGCAGTAGCGTATCGTTCTG-3'	5'-/56-FAM/AGCGCCCGG/ZEN/ATAGAGTACTTGAGG/3IABkFQ/-3'
H1fx			
	5'-AGTAAGCACTACAGCCTTCAAG-3'	5'-GCACGTCATAGAGGTAGAACTG-3'	5'-/56-FAM/CCACCGAAT/ZEN/ATGGACAACGCAATGG/3IABkFQ/-3'
Hmcn1			
	5'-AGAGTTCTTCAATGGCAAGGAG-3'	5'-ATCAAGCAGTACCAGATCACC-3'	5'-/56-FAM/ACAGCGGCA/ZEN/CCATAGGCTACAG/3IABkFQ/-3'
Hspa5			
	5'-GATGACAGCAACTTCCTCAGT-3'	5'-AGACAGACCAGAGACTCCAAT-3'	5'-/56-FAM/AGAGCAGCC/ZEN/AGAGTATGATTCCACAGA/3IABkFQ/-3'
Ism1			
	5'-GCAAGACCTACACCAAGAGC-3'	5'-CTTCCAGCCGCATCCTTC-3'	5'-/56-FAM/TGCGTACAC/ZEN/ACACAGGTGAGAAGC/3IABkFQ/-3'
Klf2			
	5'-GTTCTATGCACGATTCCTCAGT-3'	5'-ATGGAAGGCGGAATGTCTG-3'	5'-/56-FAM/AAGGTTCCC/ZEN/TGTGCTTCACCATCTT/3IABkFQ/-3'
Lars2			
	5'-TCACATTTTCACCAGCCACTA-3'	5'-CTTCGACACCTCATTGATGATCT-3'	5'-/56-FAM/ACCGATTCT/ZEN/CTTTGCCTCTTGCTTCA/3IABkFQ/-3'
Manf			
	5'-AGATGAGACCCTGTGACCAG-3'	5'-AAATGACCCCATCGAACACA-3'	5'-/56-FAM/CGCAGACCC/ZEN/CAACAACCAGACT/3IABkFQ/-3'
Nov			
	5'-GCCTTCATCCATTCTTTGCC-3'	5'-GCTTCATGTTCATTGCACTCAT-3'	5'-/56-FAM/CCCTGAACT/ZEN/CATCTGCAACGTCCTG/3IABkFQ/-3'
Phc3			
	5'-CTGTTCTTAGATGTTTGCTCGTC-3'	5'-GTCCACTTCAGACATCAGATCA-3'	5'-/56-FAM/TGCACGGCT/ZEN/CTGTTCTTCCAGG/3IABkFQ/-3'
Pknox1			
	5'-CGACTACGAACCCAACACAG-3'	5'-AGAGAATCCACCATTTGACTGAG-3'	5'-/56-FAM/ATAGCTGGT/ZEN/CCCCCTCCACATAGA/3IABkFQ/-3'
Rasl11a			
	5'-GAACGTGGCCGAGGTTG-3'	5'-AGACAATTCCATCAGCCTTAGC-3'	5'-/56-FAM/TCATCTGAC/ZEN/TCGCCCATCCTGC/3IABkFQ/-3'
Rps21			
	5'-AGTTCTCCTCGCTCGCA-3'	5'-CCGTGGTGATTTATAGCATCC-3'	5'-/56-FAM/CCAGGCGCT/ZEN/TTTTCTTGTGTTTCCT/3IABkFQ/-3'
Rps27			

 doi:10.20944/preprints202506.2250.v1

	5'-	5'-	5'-/56-
Sdf2l1	TCGCCGCTATCCAACA	CCCAGAACATCGGACTG	FAM/TCATCACCC/ZEN/TCACCGTCTTCC
	AC-3'	TC-3'	C/3IABkFQ/-3'
	5'-	5'-	5'-/56-
Sod3	GGCAACTCAGAGGCTC	GTAGCAAGCCGTAGAAC	FAM/TTTCCCTCT/ZEN/GGTGAAGTTCAG
	TTC-3'	AAGA-3'	GCC/3IABkFQ/-3'
	5'-	5'-	5'-/56-
Trem2	GACCTCTCCACCAGTTT	GCTTCAAGGCGTCATAA	FAM/TCCCAAGCC/ZEN/CTCAACACCAC
	CTC-3'	GTACA-3'	G/3IABkFQ/-3'
	5'-	5'-	5'-/56-
Trpc6	CTGGCTCTCATATACTG	TCAGCTGCATTCATGACG	FAM/AGGAGGCTG/ZEN/CGTGTGCTACA
	GTGTG-3'	AG-3'	AA/3IABkFQ/-3'
	5'-	5'-	5'-/56-
Vstm2l	ACTACCTGGCACTTTTC	ATCTCTACATCCTCGCCT	FAM/CCGGACACG/ZEN/CACTCTTCACA
	CTG-3'	GT-3'	GA/3IABkFQ/-3'
	5'-	5'-	5'-/56-
Gapdh	AATGGTGAAGGTCGGT	GTGGAGTCATACTGGAA	FAM/TGCAAATGG/ZEN/CAGCCCTGGTG/
	GTG-3'	CATGTAG-3'	3IABkFQ/-3'

Table 2. The top 50 DEGs in each comparison, ranked by absolute log_2 FC magnitude.

IH/Contorl			SH/Control			IH/SH		
Gene	**log2FC**	**P-Value**	**Gene**	**log2FC**	**P-Value**	**Gene**	**log2FC**	**P-Value**
Cebpb	-1.993	6.666E-06	*Phc3*	1.843	5.262E-07	*Phc3*	-1.545	1.708E-03
Fos	-1.644	5.295E-04	*Gng13*	-1.726	7.609E-05	*Cebpb*	-1.373	1.165E-05
Plin4	1.441	3.014E-03	*Npas4*	-1.492	3.315E-04	*H3c14*	-1.317	1.381E-02
Npas4	-1.349	9.500E-03	*Cysrt1*	-1.346	2.177E-05	*Map3k6*	1.086	7.855E-03
C2cd4b	-1.296	2.150E-04	*Plin4*	1.323	9.619E-04	*Hspb1*	1.009	1.044E-03
Rps27rt	-1.249	3.471E-02	*Egr4*	-1.295	2.606E-03	*Dynlt1f*	-0.929	1.321E-03
Hmcn1	-1.209	6.247E-03	*Pcdha11*	-1.290	5.937E-03	*Gng13*	0.901	2.744E-03
Cysrt1	-1.201	3.383E-04	*Ankub1*	1.182	1.129E-03	*Rpl17-ps8*	-0.895	4.822E-04
H1f10	-1.195	6.248E-07	*C2cd4b*	-1.181	9.489E-04	*Rpl39*	-0.886	2.877E-05
Hbb-bt	-1.187	1.340E-02	*Enho*	-1.174	4.272E-05	*Snurf*	-0.857	8.045E-03
Arc	-1.181	1.848E-02	*Ier2*	-1.145	8.485E-04	*Moap1*	0.856	3.136E-02
Pknox1	1.181	2.139E-03	*Junb*	-1.114	5.181E-04	*Phospho1*	0.844	2.287E-03
Junb	-1.172	1.515E-04	*Fos*	-1.104	2.005E-04	*Gnpnat1*	-0.836	4.827E-02
Egr2	-1.153	3.605E-02	*Gm1673*	-1.103	1.217E-03	*Rps21*	-0.788	1.248E-05
Btg2	-1.121	5.394E-04	*Slc18a2*	1.093	3.518E-03	*Tnfsf10*	-0.766	1.568E-02
Pla2g4e	-1.115	4.045E-03	*Btg2*	-1.093	1.799E-04	*Hspa1b*	0.759	1.929E-03
Egr4	-1.107	2.171E-03	*Zic4*	1.084	4.950E-02	*Gm13304*	-0.740	1.380E-02
Sdf2l1	1.067	7.463E-04	*Inhba*	1.064	1.554E-03	*Gm13306*	-0.740	1.525E-02
Slc18a2	1.062	6.197E-03	*Gm44126*	1.060	1.597E-02	*Rpl17*	-0.738	1.073E-02

 doi:10.20944/preprints202506.2250.v1

Adrb1	-1.055	6.714E-05	*Arc*	-1.047	2.575E-02	*Gm10591*	-0.737	6.057E-03
Tmem238	-1.049	2.205E-04	*Pknox1*	1.016	4.399E-03	*Ccl21b*	-0.736	1.243E-02
Ier2	-1.042	2.628E-03	*Mrpl52*	-1.010	5.217E-07	*Gm20498*	-0.724	5.646E-03
Dusp1	-1.038	8.774E-04	*Rasl11a*	-1.005	4.835E-04	*Hmgcs2*	-0.716	7.510E-04
Rasl11a	-1.031	9.329E-04	*Pcsk1n*	-0.990	1.870E-05	*Rnasek*	0.704	4.290E-02
Ism1	-1.025	1.550E-03	*Tmem238*	-0.987	8.084E-04	*Dcst1*	-0.701	4.809E-02
Vstm2l	-1.021	6.329E-06	*Wnt9a*	-0.979	1.821E-03	*Pcdha3*	-0.699	2.567E-03
Ankub1	1.004	3.126E-02	*Tnfaip6*	0.965	1.090E-02	*U2af1l4*	-0.698	1.711E-02
Zfp708	0.990	1.405E-02	*Oxld1*	-0.963	1.739E-02	*Hexim2*	0.687	1.335E-03
Tusc1	-0.989	3.795E-03	*Dnah12*	0.938	2.121E-02	*Gstp-ps*	-0.665	2.933E-03
Adamts16	-0.983	6.563E-03	*Apold1*	-0.928	4.507E-02	*2300009A05Rik*	0.664	3.020E-02
Inhba	0.980	1.889E-03	*Mrpl54*	-0.926	8.988E-04	*Itm2a*	-0.657	9.970E-06
Lamc2	0.973	4.439E-02	*Prrg1*	0.919	5.807E-03	*Adrb1*	-0.657	8.013E-04
Pcdhgb5	-0.961	1.859E-02	*Phospho1*	-0.918	3.473E-03	*Lfng*	0.654	2.993E-03
Iqschfp	-0.955	2.146E-02	*Gm2423*	-0.911	9.762E-04	*Dbi*	0.654	4.166E-05
Ccl21b	-0.955	2.696E-03	*S100a13*	-0.910	1.517E-04	*Rps28*	-0.648	5.831E-04
Peg10	0.935	1.883E-02	*Rps29*	-0.896	2.184E-04	*Scrg1*	-0.642	2.020E-03
Hba-a2	-0.928	1.310E-04	*Ly6h*	-0.872	2.158E-03	*Adamts16*	-0.642	4.729E-02
Gm13889	-0.916	1.187E-05	*Trnp1*	-0.868	9.911E-05	*Hspa1a*	0.641	2.541E-03
Sap30l	-0.913	1.711E-04	*Klf2*	-0.864	4.240E-03	*Mrpl54*	0.639	1.883E-03
Plekhg4	0.905	5.845E-03	*Myl6b*	-0.856	5.866E-04	*Ptpn6*	0.639	8.596E-03
Gm10591	-0.894	1.155E-02	*Sap30l*	-0.852	5.689E-06	*Peg10*	0.636	4.555E-02
Fbxl9	-0.886	5.532E-06	*Erf*	-0.844	5.686E-04	*Rtl3*	0.635	2.598E-02
Wnt9a	-0.866	4.959E-03	*Tmem160*	-0.843	2.832E-03	*Fancd2*	-0.631	1.993E-02
Frat2	-0.861	4.246E-03	*Sox18*	-0.842	1.348E-02	*Ror1*	-0.626	9.413E-03
Sts	-0.855	8.503E-04	*Rpl38*	-0.840	2.093E-05	*Otogl*	-0.624	1.961E-02
Insm1	-0.844	5.657E-04	*Tmem256*	-0.840	1.783E-04	*Rpl22l1*	-0.624	2.989E-04
Hspb1	0.843	1.663E-02	*Tead3*	-0.840	5.864E-03	*Lars2*	-0.619	4.500E-03
Tomm6	-0.838	2.268E-03	*Zfp524*	-0.836	1.869E-03	*Nadsyn1*	-0.614	1.815E-02
Arf6	-0.837	1.101E-06	*Hcfc1r1*	-0.829	1.688E-06	*Cdk2ap2*	0.611	2.685E-03
Pgam2	-0.836	1.671E-02	*Chchd10*	-0.822	2.469E-04	*Ppara*	-0.608	2.653E-02

2.3. Functional enrichment analysis

Gene Ontology (GO) enrichment analysis using Metascape revealed significantly altered biological processes associated with DEGs patterns (Figure 3). For DEGs in the IH vs. control comparison, enriched processes included neurological functions such as learning or memory (GO: 0007611, $-\log_{10}$ (P) = 3.86) and brain development (GO: 0007420, $-\log_{10}$ (P) = 2.96), as well as response to reactive oxygen species (GO: 0000302, $-\log_{10}$ (P) = 3.17), blood vessel development (GO: 0001568, $-\log_{10}$ (P) = 3.34), and IL-17 signaling pathway (mmu04657, $-\log_{10}$ (P) = 2.75) (Figure 3A). In contrast, DEGs in the SH vs. control comparison showed enrichment only in response to hypoxia (GO: 0001666, $-\log_{10}$ (P) = 2.22) with no effects on learning or memory (Figure 3B). The IH vs. SH comparison also revealed no enrichment in learning or memory (Figure 3C).

 doi:10.20944/preprints202506.2250.v1

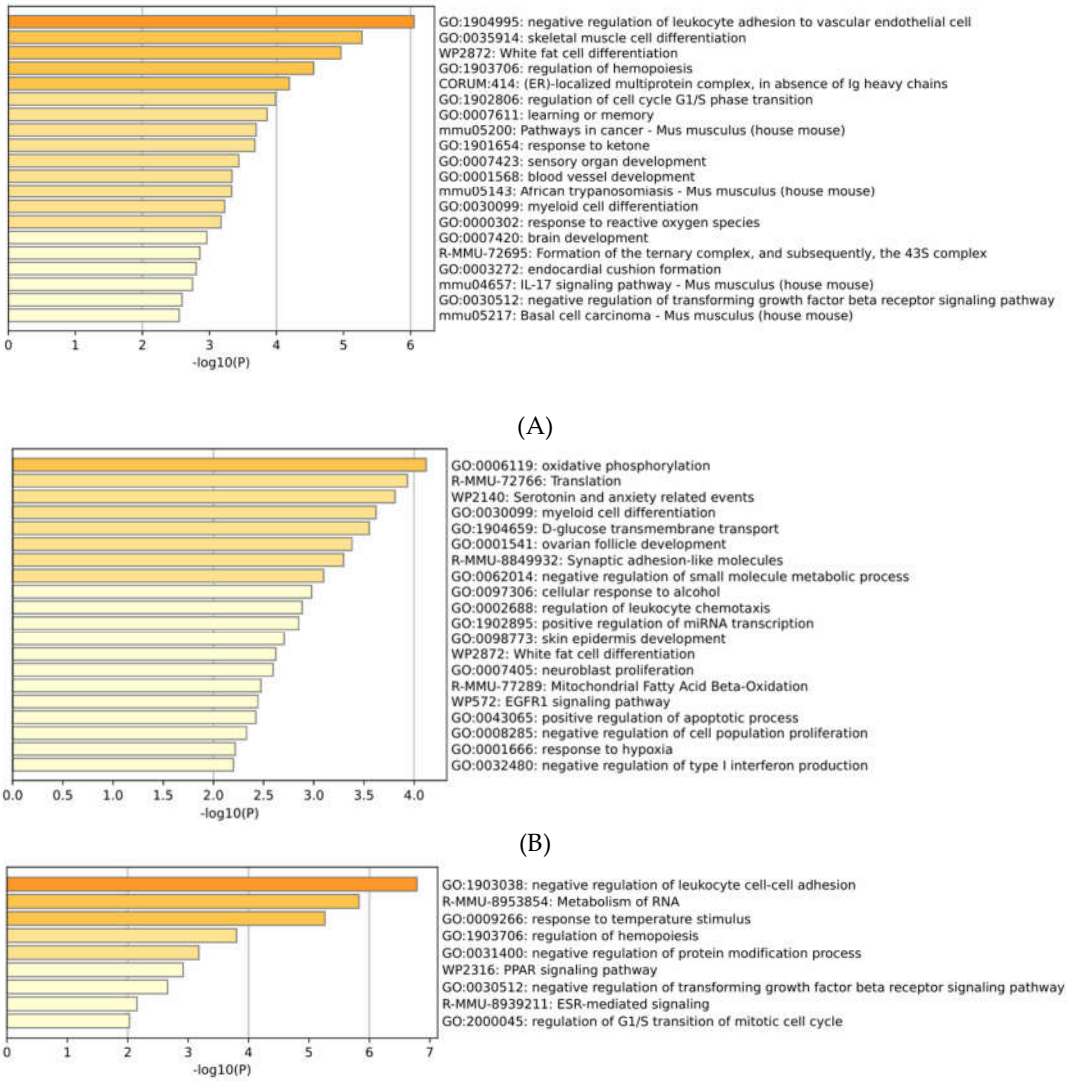

Figure 3. Gene Ontology (GO) analysis of biological processes (Control: n = 4, IH and SH: n = 5 each). (A) GO analysis results for DEGs in the IH vs. control comparison. The X-axis shows -log10(P) values. In addition to neurological processes such as learning or memory and brain development, response to reactive oxygen species and blood vessel development showed significant enrichment. (B) GO analysis results for DEGs in the SH vs. control comparison. Enrichment in response to hypoxia was observed, but no significant enrichment in learning, memory, or neurological processes was found. (C) GO analysis results for DEGs in the IH vs. SH comparison. No significant enrichment in neurological processes was observed. Statistical significance was set at $P < 0.05$.

QIAGEN Ingenuity Pathway Analysis (IPA) (QIAGEN, Hilden, Germany) identified major molecular pathways altered in each comparison. Results are displayed as positive or negative Z-scores indicating activation and inhibition, respectively. Figures 4A and B show the top 20 activated and inhibited pathways in the IH group compared to controls, respectively. Activated pathways included mitochondrial dysfunction ($-\log_{10}$ (P) = 19.6, Z-score = 4.838), while inhibited pathways included the KEAP1-NFE2L2 antioxidant pathway ($-\log_{10}$ (P) = 5.74, Z-score = -5.303). For the IH vs. SH comparison, the top 20 altered pathways are shown in Figures 4C and D, with the KEAP1-NFE2L2 pathway inhibited ($-\log_{10}$ (P) = 4.33, Z-score = -3.441).

 doi:10.20944/preprints202506.2250.v1

Figure 4. QIAGEN Ingenuity Pathway Analysis (QIAGEN IPA) results showing altered molecular pathways (Control: n = 4, IH and SH: n = 5 each). (A) Major molecular pathways activated in the IH group compared to the control group. Pathways such as mitochondrial dysfunction were activated. (B) Major molecular pathways inhibited in the IH group compared to the control group. The KEAP1-NFE2L2 antioxidant pathway was inhibited. (C) Major molecular pathways activated in the IH group compared to the SH group. (D) Major molecular pathways inhibited in the IH group compared to the SH group. The KEAP1-NFE2L2 antioxidant pathway was inhibited. The X-axis shows -$\log_{10}$ (P-value) and the color scale shows activation Z-score, with red indicating activation and blue indicating inhibition. Statistical significance was set at -$\log_{10}$ (P) > 1.3 and |Z-score| > 2.0. IH, intermittent hypoxia; SH, sustained hypoxia.

2.4. RT-qPCR

mRNA expression changes obtained by RT-qPCR are shown in Figure 5 and Table 3. Of the 23 genes analyzed, 19 genes showed no statistically significant effects of exposure conditions, including *Adrb1*, *Foxo6*, *Trem2*, *Klf2*, *Sod3*, *Cebpb*, *Dbi*, *Manf*, *Trpc6*, *Hspa5*, *Nov*, *Basp1*, *H1fx*, *Ism1*, *Phc3*, *Pknox1*, *Rasl11a*, *Rps27*, and *Sdf2l1*.

Four genes showed significant expression changes: *Lars2* ($F(2,22) = 4.376$, $P = 0.025$), *Rps21* ($F(2,22) = 3.870$, $P = 0.036$), *Hmcn1* ($F(2,22) = 9.196$, $P = 0.001$), and *Vstm2l* ($F(2,22) = 5.509$, $P = 0.012$). Post-hoc analysis using Tukey's HSD test revealed the following patterns: *Lars2* expression was significantly lower in the IH group compared to the SH group ($P = 0.036$) with a trend toward decrease vs. control ($P = 0.056$). *Rps21* expression was significantly lower in the SH group compared

 doi:10.20944/preprints202506.2250.v1

to control (P = 0.033). *Hmcn1* expression was significantly lower in the IH group compared to both control (P = 0.008) and SH groups (P = 0.002). *Vstm2l* expression was significantly lower in the IH group compared to control (P = 0.012) with a trend toward decrease vs. SH (P = 0.055).

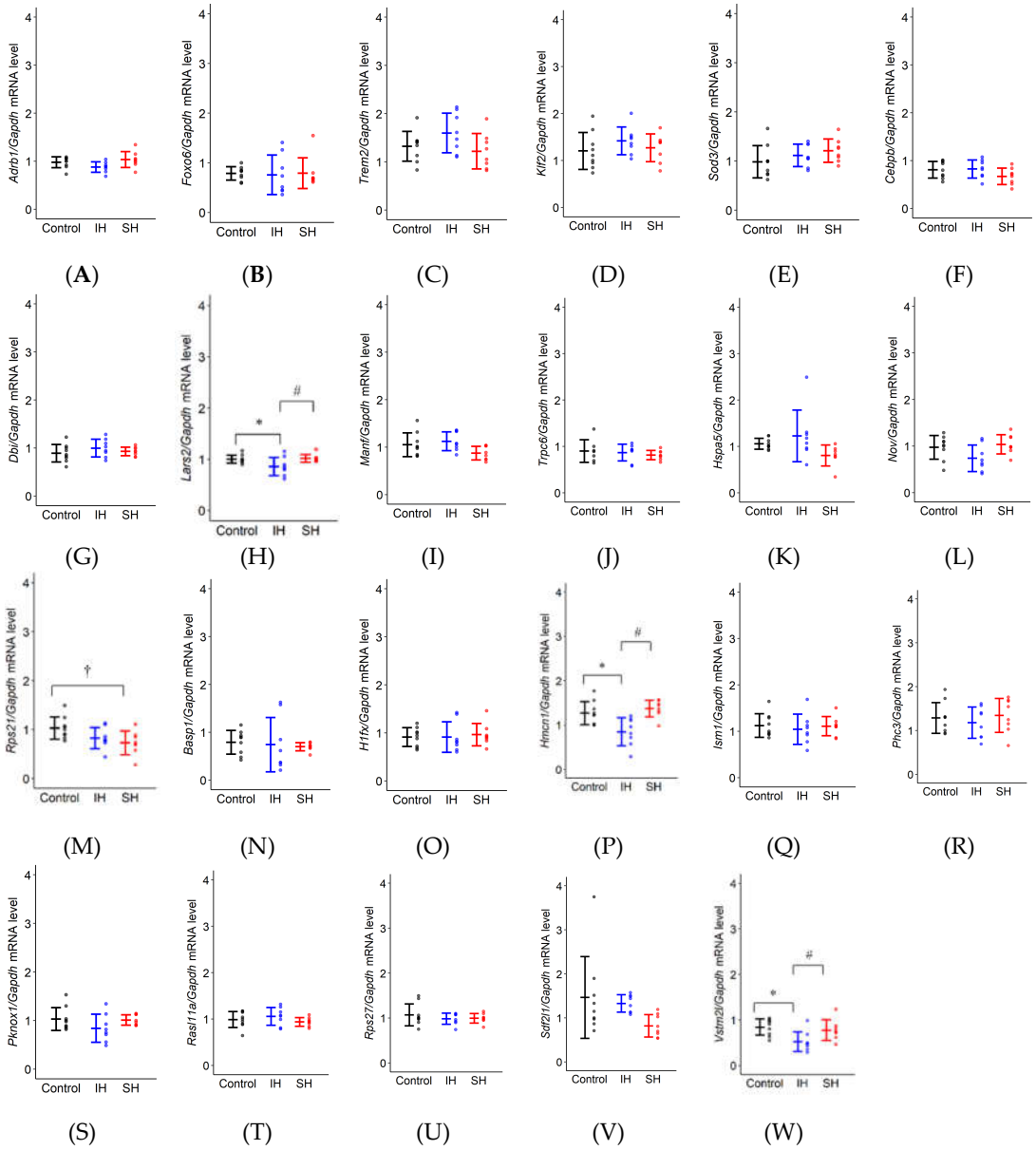

Figure 5. Adrb1, Foxo6, Trem2, Klf2, Sod3, Cebpb, Dbi, Lars2, Manf, Trpc6, Hspa5, Nov, Rps21, Basp1, H1fx, Hmcn1, Ism1, Phc3, Pknox1, Rasl11a, Rps27, Sdf2l1, and Vstm2l (A-W) mRNA expression in mouse hippocampus. Values are presented as mean ± standard error (Control: n = 9, IH and SH: n = 8 each). (H) Lars2 mRNA in the IH group showed a significant decrease compared to the SH group (# P = 0.036) and a trend toward decrease compared to the control group (P = 0.056). (M) Rps21 mRNA in the SH group showed a significant decrease compared to the control group († P = 0.033). (P) Hmcn1 mRNA in the IH group showed a significant decrease compared to both the control group (* P = 0.008) and the SH group (# P = 0.002). (W) Vstm2l mRNA in the IH group showed a significant decrease compared to the control group (* P = 0.012) and a trend toward decrease compared to the SH group (P = 0.055). Statistical analysis was performed using one-way ANOVA followed by Tukey's HSD test. * P < 0.05 vs. control; # P < 0.05, IH vs. SH; † P < 0.05, SH vs. control. Statistical significance was set at P < 0.05. IH, intermittent hypoxia; SH, sustained hypoxia.

 doi:10.20944/preprints202506.2250.v1

Table 3. RT-qPCR results for mRNA expression levels.

Gene	F value	LS mean	IH vs Control	SH vs Control	IH vs SH
		Control : 0.977±0.064			
Adrb1	F(2,22) = 2.915, P = 0.075	IH : 0.877±0.066	P = 0.277	P = 0.662	P = 0.066
		SH : 1.033±0.066			
		Control : 0.786±0.144			
Foxo6	F(2,22) = 0.029, P = 0.971	IH : 0.758±0.148	P = 0.979	P = 0.999	P = 0.973
		SH : 0.791±0.148			
		Control : 1.321±0.176			
Trem2	F(2,22) = 2.343, P = 0.120	IH : 1.597±0.181	P = 0.282	P = 0.831	P = 0.116
		SH : 1.218±0.181			
		Control : 1.202±0.163			
Klf2	F(2,22) = 0.899, P = 0.421	IH : 1.417±0.168	P = 0.400	P = 0.912	P = 0.656
		SH : 1.269±0.168			
		Control : 0.984±0.132			
Sod3	F(2,22) = 1.495, P = 0.246	IH : 1.114±0.135	P = 0.588	P = 0.222	P = 0.765
		SH : 1.209±0.135			
		Control : 0.808±0.087			
Cebpb	F(2,22) = 1.808, P = 0.188	IH : 0.823±0.089	P = 0.984	P = 0.271	P = 0.223
		SH : 0.670±0.089			
		Control : 0.892±0.078			
Dbi	F(2,22) = 0.930, P = 0.409	IH : 0.997±0.080	P = 0.384	P = 0.891	P = 0.668
		SH : 0.928±0.080			
		Control : 0.999±0.058			
Lars2	F(2,22) = 4.376, *P = 0.025	IH : 0.857±0.059	P = 0.056	P = 0.954	*P = 0.036
		SH : 1.016±0.059			
		Control : 1.051±0.099			
Manf	F(2,22) = 3.191, P = 0.061	IH : 1.123±0.102	P = 0.753	P = 0.194	P = 0.057
		SH : 0.872±0.102			
		Control : 0.900±0.094			
Trpc6	F(2,20) = 0.452, P = 0.643	IH : 0.866±0.090	P = 0.932	P = 0.624	P = 0.822
		SH : 0.812±0.090			
		Control : 1.057±0.177			
Hspa5	F(2,21) = 2.733, P = 0.088	IH : 1.226±0.182	P = 0.591	P = 0.340	P = 0.073
		SH : 0.802±0.182			
		Control : 0.973±0.120			
Nov	F(2,22) = 2.310, P = 0.123	IH : 0.738±0.123	P = 0.145	P = 0.987	P = 0.207
		SH : 0.954±0.123			
		Control : 1.029±0.111			
Rps21	F(2,22) = 3.870, *P = 0.036	IH : 0.826±0.114	P = 0.182	*P = 0.033	P = 0.676
		SH : 0.729±0.114			

 doi:10.20944/preprints202506.2250.v1

		Control : 0.792±0.173			
Basp1	F(2,22) = 0.151, P = 0.861	IH : 0.741±0.178	P = 0.953	P = 0.849	P = 0.967
		SH : 0.697±0.178			
		Control : 0.912±0.122			
H1fx	F(2,22) = 0.110, P = 0.897	IH : 0.913±0.125	P = 1.000	P = 0.909	P = 0.916
		SH : 0.963±0.125			
		Control : 1.271±0.126			
Hmcn1	F(2,22) = 9.196, *P = 0.001	IH : 0.849±0.130	*P = 0.008	P = 0.703	*P = 0.002
		SH : 1.373±0.130			
		Control : 1.122±0.130			
Ism1	F(2,22) = 0.204, P = 0.817	IH : 1.044±0.134	P = 0.821	P = 0.995	P = 0.875
		SH : 1.110±0.134			
		Control : 1.286±0.177			
Phc3	F(2,22) = 0.423, P = 0.660	IH : 1.179±0.182	P = 0.819	P = 0.943	P = 0.643
		SH : 1.344±0.182			
		Control : 1.030±0.109			
Pknox1	F(2,22) = 1.774, P = 0.193	IH : 0.840±0.112	P = 0.212	P = 0.980	P = 0.306
		SH : 1.010±0.112			
		Control : 0.988±0.077			
Rasl11a	F(2,22) = 1.129, P = 0.342	IH : 1.057±0.079	P = 0.652	P = 0.795	P = 0.312
		SH : 0.938±0.079			
		Control : 1.067±0.084			
Rps27	F(2,22) = 0.640, P = 0.537	IH : 0.993±0.086	P = 0.570	P = 0.642	P = 0.993
		SH : 0.984±0.086			
		Control : 1.464±0.286			
Sdf2l1	F(2,22) = 2.764, P = 0.085	IH : 1.327±0.295	P = 0.882	P = 0.084	P = 0.218
		SH : 0.818±0.295			
		Control : 0.840±0.100			
Vstm2l	F(2,22) = 5.509, *P = 0.012	IH : 0.521±0.103	*P = 0.012	P = 0.799	P = 0.055
		SH : 0.775±0.103			

Asterisks indicate statistical significance: *P < 0.05. Statistical analysis was performed using one-way ANOVA. Tukey's HSD test was conducted to examine differences between groups.

3. Discussion

The present study demonstrates that IH induces learning or memory impairments. RNA-seq and RT-qPCR analyses indicated the involvement of the KEAP1-NFE2L2 pathway and identified novel genes potentially associated with OSAS.

Behavioral tests demonstrated that IH specifically induces cognitive dysfunction. The passive avoidance test revealed significant learning or memory impairments in the IH group, with a decreased proportion of mice exceeding the cutoff value compared to both control and SH groups, while no difference was observed between SH and control groups. These findings are consistent with previous research using similar IH conditions (minimum FiO_2 5%/4-minute cycles/8 hours daily/3 weeks) [16] and clearly indicate that intermittent, rather than sustained, hypoxia specifically impairs cognitive function. Although the Y-maze test showed no significant differences between groups

 doi:10.20944/preprints202506.2250.v1

under our 4-week experimental conditions, this aligns with previous studies [16], and longer exposure durations may be required for spatial cognitive impairment [15].

RNA-seq analysis identified DEGs among groups. GO analysis of RNA-seq data revealed alterations in "learning or memory" and "response to reactive oxygen species" as key categories specifically altered in the IH group. Based on these results, RT-qPCR analysis revealed significant downregulation in four genes: *Lars2*, *Hmcn1*, *Vstm2l*, and *Rps21*. *Lars2*, encoding mitochondrial leucyl-tRNA synthetase essential for mitochondrial protein synthesis and functional maintenance [20–23], has been linked to Alzheimer's disease, with knockout mice exhibiting cognitive dysfunction, increased p-tau, and hippocampal atrophy [24]. Additionally, decreased *Lars2* expression impairs mitochondrial stress responses, leading to elevated ROS levels [25]. *Hmcn1*, encoding an extracellular protein involved in epithelial cell junction organization [26], has been implicated in Alzheimer's disease pathways [27]. *Vstm2l* is localized to mitochondria and involved in maintaining mitochondrial homeostasis [28]. The previous study showed that repeated cycles of hypoxia-reoxygenation increased ROS production [17]. In addition, the increase in mitochondrial ROS is associated with neuronal cell death and cognitive dysfunction [18,19]. Therefore, the downregulation of mitochondrial genes *Lars2* and *Vstm2l* may have contributed to cognitive dysfunction through impaired mitochondrial function and elevated ROS levels. In contrast, *Rps21*, encoding ribosomal protein S21 [29], showed downregulation specifically in the SH group, but there are few reports linking *Rps21* to cognitive dysfunction, and this downregulation may not be related to cognitive function.

Pathway analysis using QIAGEN IPA revealed significant suppression of the KEAP1-NFE2L2 pathway in both IH and SH groups compared to the control group, with stronger suppression observed in the IH group. The KEAP1-NFE2L2 pathway functions as a major regulator of intracellular antioxidant defense systems, playing cytoprotective roles including suppression of inflammatory signals [30], regulation of mitochondrial function [31], prevention of cell death [32], and neuroprotection [33]. Chronic IH exposure has been shown to decrease *Nrf2* expression in multiple organs, including the hippocampus [13]. In the present study, although *Nrf2* expression showed no significant differences between groups, pathway analysis revealed alterations in the KEAP1-NFE2L2 pathway. IH-induced suppression of the KEAP1-NFE2L2 pathway may have attenuated antioxidant defense and neuroprotective mechanisms, contributing to cognitive dysfunction.

This study has limitations including limited validation of protein-level expression and functional involvement of the identified genes. Further studies are needed to elucidate the specific mechanisms by which these genes contribute to cognitive dysfunction and to validate their functional roles in OSAS-related cognitive impairment.

4. Materials and Methods

4.1. Animals

Seventy-one male C57BL/6J mice (weight: 22.5 ± 2.9 g; age: 8 weeks; Japan SLC, Hamamatsu, Japan) were used for behavioral and molecular analyses. Mice were housed in groups of 5–6 per cage (30 cm length × 20 cm width × 12 cm height) under controlled environmental conditions at a temperature of 24 ± 1°C and a 12:12-hour light-dark cycle (lights on at 08:00). Mice had ad libitum access to food and water. All experimental protocols were approved by the Animal Research Committee of Showa Medical University (Tokyo, Japan) (approval number: 124040).

4.2. Experimental protocol

Mice were allocated to the control group (n = 38), IH group (n = 16), and SH group (n = 17). The IH group mice were exposed to intermittent hypoxic loading with alternating oxygen concentrations of 10% and 21% in 2-minute cycles for 8 hours daily (12:00–20:00). The SH group mice were exposed to continuous hypoxic loading at 10% oxygen concentration for 8 hours daily (12:00–20:00). The

 doi:10.20944/preprints202506.2250.v1

control group mice were housed without hypoxic exposure. Mice were maintained under these conditions for 28 days, followed by Y-maze testing on day 29, passive avoidance testing (day 1) on day 29, and passive avoidance testing (day 2) on day 30. After behavioral experiments, mice were euthanized under isoflurane anesthesia and decapitated for hippocampal collection. Hippocampi were immersed in RNA stabilization solution (RNAprotect Tissue Reagent, QIAGEN) to prevent RNA degradation, kept at 4°C overnight, and then stored at -80°C. Hippocampal samples were used for RNA-seq and cDNA synthesis.

4.3. Intermittent hypoxia exposure, sustained hypoxia exposure

Mice in the IH group were exposed to intermittent hypoxia for 8 hours daily from 12:00 to 20:00 for 28 days using a custom-made gas control delivery system (Shibata Scientific Technology Ltd., Tokyo, Japan) with oxygen and nitrogen alternation to create alternating hypoxic and normoxic conditions, controlled by a pressure controller (Gas Cylinder Auto Changer Model 8500, WAKEN BTECH CO., LTD., Kyoto, Japan). One cycle was defined as 120 seconds, consisting of a hypoxic phase (10% oxygen, 70 seconds) and a normoxic phase (21% oxygen, 50 seconds). Oxygen concentrations were continuously monitored by an oxygen analyzer (XP-3380 Ⅱ, Shin-Cosmos Electric Co., Ltd., Osaka, Japan) and recorded using an A/D converter (PL2604 PowerLab 4/26, ADInstruments, Dunedin, New Zealand) connected to LabChart v7 (ADInstruments).

Mice in the SH group were housed using a custom-made acrylic box (56 cm width × 45 cm height × 41 cm depth) (Kyodo International Co., Ltd., Kawasaki, Japan) with their cages placed inside. The box featured five 0.8 cm air holes: two at the upper corners of the back panel and two at the lower corners of each side panel, with a fan attached at a height of 28 cm on the left side panel that operated continuously throughout the experiment. A gas control delivery system (ProOx P110, BioSpherix, Parish, NY, USA) and a pressure controller (Gas Cylinder Auto Changer Model 8500, WAKEN BTECH CO., LTD.) were employed to maintain hypoxic conditions using nitrogen. The system continuously monitored oxygen concentration using a built-in oxygen analyzer and featured a programmable timer function (H5S, OMRON, Kyoto, Japan). Mice were exposed to sustained hypoxia at 10% oxygen concentration for 8 hours daily (12:00-20:00) over 28 days. During the remaining period (20:00-12:00), atmospheric oxygen concentration (21%) was maintained using an air pump (AP-30P, Yasunaga Air Pump Co., Ltd., Tokyo, Japan).

Both gas delivery systems were validated before experiments and underwent regular calibration to ensure accurate gas circulation and maintain stable concentrations.

4.4. Y-maze test

Based on previous studies [15,16,34], mouse short-term spatial working memory was evaluated using the Y-maze test. Forty-nine mice (control group: n = 17, IH group: n = 16, SH group: n = 17) were analyzed, with one mouse from the IH group excluded due to deviation from the Y-maze test during the experiment. The maze consisted of three identical arms radiating from a central area at 120° angles to each other, with dimensions of 40 cm length × 12 cm height, 3 cm width at the floor expanding to 10 cm width at the ceiling. Arm entry was defined as all four paws completely entering an arm. Mice explored the maze for 8 minutes while the number of arm entries was recorded by an overhead video camera (MX Brio C1100PG, Logitech International S.A., Lausanne, Switzerland) and analyzed using behavioral analysis software (SMART V 3.0, Bio Research Center Co., Ltd., Nagoya, Japan). The percentage of spontaneous alternation was calculated as: %Alternations = (number of triads/(N-2)) × 100, where N = total number of entries.

4.5. Passive avoidance test

Based on previous studies [16,35], mouse memory and learning ability were evaluated using a two-compartment step-through passive avoidance apparatus (MPB-M030, Melquest Co., Toyama, Japan). Seventy-one mice (control group: n = 38, IH group: n = 16, SH group: n = 17) were initially

 doi:10.20944/preprints202506.2250.v1

used. The apparatus consisted of a bright compartment (10.0 × 18.0 × 14.5 cm) and a dark compartment (18.0 × 18.0 × 14.5 cm) separated by a wall with a guillotine door. The bright compartment was illuminated at 145 lx.

During the training phase, mice were placed in the bright compartment for 20 seconds before the guillotine door was opened to allow entry into the dark compartment. When mice entered the dark compartment, the guillotine door was closed and an electric shock (0.3 mA) was delivered for 3 seconds. Testing was performed 24 hours after training. Mice were placed in the bright compartment for 20 seconds before the guillotine door was opened. The latency to enter the dark compartment was recorded for up to 300 seconds. Mice that did not enter the dark compartment after 300 seconds were considered to have retained memory, and this proportion was used for analysis. Due to experimental protocol errors, 11 mice (6 from the control group and 5 from the IH group) that received multiple electrical stimulations were excluded from the analysis, resulting in final group sizes of n = 32 (control), n = 11 (IH), and n = 17 (SH).

4.6. RNA sequencing

Total RNA was extracted from hippocampi using the RNeasy® Plus Universal Mini Kit (QIAGEN) following the manufacturer's protocol. Total RNA concentration and purity were determined based on the ratio of absorbance at 260 nm and 280 nm using a NanoDrop One Spectrophotometer (Thermo Fisher Scientific, Waltham, MA, USA). For RNA-seq analysis, 5 samples each from the IH and SH groups and 4 samples from the control group were submitted to Rhelixa Co., Ltd. (Tokyo, Japan). Control samples were prepared from mice exposed to atmospheric conditions under identical experimental conditions (same mouse strain, age, and housing duration) in a preliminary experiment.

In the primary analysis, adapter sequences and low-quality bases in paired-end reads were removed with fastp (version 0.23.4). Filtered paired-end reads were mapped to the mouse reference genome (GRCm39) by HISAT2 (version 2.2.1) and expression levels were quantified by StringTie (version 2.2.1). The read count values of the gene expression data (raw signal) were subjected to appropriate processing by Subio Platform (Subio Inc, Nagoya, Japan), including binary log transformation, global normalization by 80th percentile, low signal cutoff (read counts < 40), missing value completion ($\log_2$ 32), correction by control group values (Processed signal), averaging and ratio calculation to the control group by exponential function (FC). Specifically, among the read gene expression data (40015 genes), only genes for which raw signal in each group was above the low signal cutoff value for protein-coding genes were extracted (13733 genes), further filtered to genes with Processed signal ≥ |0.25| (7756 genes).

For secondary analysis, functional analysis was performed using Metascape to identify enriched biological pathways and processes [36]. DEGs lists were analyzed with thresholds of FC > 1.5 or < 0.67 and significance level $P < 0.05$. Furthermore, pathway analysis was conducted using QIAGEN IPA to examine molecular networks. Of the 7756 genes, 38 genes that were not mapped within the QIAGEN IPA were excluded, and of the remaining 7718 genes, those meeting $P < 0.05$ were analyzed. Data were considered significant with thresholds of $-\log_{10}(P) > 1.3$ and |Z-score| > 2.0. The sequence data were deposited in the Gene Expression Omnibus database (https://www.ncbi.nlm.nih.gov/geo; accession no. GSE 299437).

4.7. RT-qPCR

For RT-qPCR analysis, total RNA samples from the control group included 9 samples extracted in this experiment, while the IH and SH groups used 8 samples from each group. cDNA was synthesized from total RNA using PrimeScript™ RT Master Mix (Takara Bio Inc., Kusatsu, Japan) according to the manufacturer's protocol.

Target genes were selected based on several criteria. Based on GO analysis results, genes with read counts >100 that have been reported to be associated with cognitive function or neural processes within the "learning or memory" and "response to reactive oxygen species" categories were selected

 doi:10.20944/preprints202506.2250.v1

(*Adrb1* [37], *Foxo6* [38], *Trem2* [39], *Klf2* [40], *Sod3* [41]). Additionally, three categories of genes were included: genes previously reported to be associated with cognitive function or neural processes but not identified in the GO analysis (*Cebpb* [42], *Dbi* [43], *Lars2* [24], *Manf* [44], *Trpc6* [45]), genes with high read counts (>1500) but no existing literature reports (*Hspa5*, *Nov*, *Rps21*), and genes with large FC (>2.0 or <0.5) (*Basp1*, *H1fx*, *Hmcn1*, *Ism1*, *Phc3*, *Pknox1*, *Rasl11a*, *Rps27*, *Sdf2l1*, *Vstm2l*).

Probe details are provided in Table 1. All probes contained 6-FAM at the 5' end, ZEN quencher internally, and Iowa Black FQ quencher at the 3' end, and were synthesized as PrimeTime Mini qPCR Assay (Integrated DNA Technologies, Inc., Coralville, IA, USA). Quantitative PCR was performed in a total volume of 10 μL with PrimeTime® Gene Expression Master Mix (Integrated DNA Technologies, Inc., Coralville, IA, USA) and QuantStudio™ 5 Real-Time PCR system (Thermo Fisher Scientific, Waltham, MA, USA) according to the manufacturer's instructions. The PCR conditions were as follows: initial denaturation at 95°C for 3 min, followed by 45 cycles of 95°C for 15 sec and 60°C for 30 sec. Relative expression levels of each gene were determined by the ΔΔCt method using *Gapdh* as an internal control.

4.8. Statistical Analysis

Statistical analyses were performed using JMP Pro ver.17.0.0 (JMP Statistical Discovery LLC, Cary, NC, USA). All data are presented as mean ± standard error. For Y-maze test alternation behavior rates and hippocampal mRNA levels, one-way analysis of variance (ANOVA) followed by Tukey's HSD test was used for multiple group comparisons. For the passive avoidance test, the proportion of mice exceeding the cutoff value (300 seconds) was compared using the chi-square test. Statistical significance was set at $P < 0.05$.

5. Conclusions

In this study, we demonstrated that IH induces learning or memory impairments using a mouse model of OSAS. RNA-seq and RT-qPCR analyses revealed three genes (*Lars2*, *Hmcn1*, and *Vstm2l*) that showed specific downregulation in the IH group and confirmed the involvement of the KEAP1-NFE2L2 antioxidant pathway. These findings provide insights into the molecular basis of cognitive dysfunction in OSAS.

Supplementary Materials: None.

Author Contributions: K.M. and Y.U. contributed equally to this work. Conceptualization, M.I.; methodology, Y.U., M.I., S.S., T.O., and T.Y.; investigation, Y.U., K.M., R.N., S.K., F.I., H.O., and Y.A.; data analysis, K.M., Y.U., M.H., Y.Y., and F.I.; writing—original draft preparation, K.M., Y.U., M.H., F.I., and H.I.; writing—review and editing, M.I.; supervision, T.Y. and M.I.; funding acquisition, M.I. All authors read and agreed to the published version of the manuscript.

Funding: This research was funded by JSPS KAKENHI, grant number 24K14685 to M.I.**Institutional Review Board Statement:** The animal study protocol was conducted in accordance with the guidelines for animal experimentation and was approved by the Animal Research Committee of Showa Medical University (protocol code: 124040, date of approval: April 1, 2024).

Informed Consent Statement: Not applicable.

Data Availability Statement: Raw data were generated at Showa Medical University. Derived data supporting the findings of this study are available from the corresponding author Y.U. upon reasonable request.

Acknowledgments: None.

Conflicts of Interest: The authors declare no conflicts of interest.

 doi:10.20944/preprints202506.2250.v1

Abbreviations

The following abbreviations are used in this manuscript:

OSAS	Obstructive sleep apnea syndrome
IH	Intermittent hypoxia
SH	Sustained hypoxia
ROS	Reactive oxygen species
RNA-seq	RNA sequencing
DEGs	Differentially Expressed Genes
FC	Fold change
GO	Gene Ontology
IPA	Ingenuity Pathway Analysis

References

1. Senaratna, C.V.; Perret, J.L.; Lodge, C.J.; Lowe, A.J.; Campbell, B.E.; Matheson, M.C.; Hamilton, G.S.; Dharmage, S.C. Prevalence of Obstructive Sleep Apnea in the General Population: A Systematic Review. *Sleep Med Rev* **2017**, *34*, 70–81. doi: 10.1016/j.smrv.2016.07.002
2. Benjafield, A.V.; Ayas, N.T.; Eastwood, P.R.; Heinzer, R.; Ip, M.S.M.; Morrell, M.J.; Nunez, C.M.; Patel, S.R.; Penzel, T.; Pépin, J.L.D.; et al. Estimation of the Global Prevalence and Burden of Obstructive Sleep Apnoea: A Literature-Based Analysis. *Lancet Respir Med* **2019**, *7*, 687–698. doi: 10.1016/S2213-2600(19)30198-5
3. Lévy, P.; Kohler, M.; McNicholas, W.T.; Barbé, F.; McEvoy, R.D.; Somers, V.K.; Lavie, L.; Pépin, J.L. Obstructive Sleep Apnoea Syndrome. *Nat Rev Dis Primers* **2015**, *1*, 15015. doi: 10.1038/nrdp.2015.15
4. Marin, J.M.; Agusti, A.; Villar, I.; Forner, M.; Nieto, D.; Carrizo, S.J.; Barbé, F.; Vicente, E.; Wei, Y.; Javier Nieto, F.; et al. Association between Treated and Untreated Obstructive Sleep Apnea and Risk of Hypertension. *JAMA* **2012**, *307*, 2169–2176. doi: 10.1001/jama.2012.3418
5. Reutrakul, S.; Mokhlesi, B. Obstructive Sleep Apnea and Diabetes: A State of the Art Review. *Chest* **2017**, *152*, 1070–1086. doi: 10.1016/j.chest.2017.05.009
6. Kato, M.; Adachi, T.; Koshino, Y.; Somers, V.K. Obstructive Sleep Apnea and Cardiovascular Disease. *Circ J* **2009**, *73*, 1363–1370. doi: 10.1253/circj.cj-09-0364
7. Bucks, R.S.; Olaithe, M.; Eastwood, P. Neurocognitive Function in Obstructive Sleep Apnoea: A Meta-Review. *Respirology* **2013**, *18*, 61–70. doi: 10.1111/j.1440-1843.2012.02255.x
8. Beebe, D.W.; Gozal, D. Obstructive Sleep Apnea and the Prefrontal Cortex: Towards a Comprehensive Model Linking Nocturnal Upper Airway Obstruction to Daytime Cognitive and Behavioral Deficits. *J Sleep Res* **2002**, *11*, 1–16. doi: 10.1046/j.1365-2869.2002.00289.x
9. Findley, L.J.; Barth, J.T.; Powers, D.C.; Wilhoit, S.C.; Boyd, D.G.; Suratt, P.M. Cognitive Impairment in Patients with Obstructive Sleep Apnea and Associated Hypoxemia. *Chest* **1986**, *90*, 686–690. doi: 10.1378/chest.90.5.686
10. Bubu, O.M.; Andrade, A.G.; Umasabor-Bubu, O.Q.; Hogan, M.M.; Turner, A.D.; de Leon, M.J.; Ogedegbe, G.; Ayappa, I.; Jean-Louis G, G.; Jackson, M.L.; et al. Obstructive Sleep Apnea, Cognition and Alzheimer's Disease: A Systematic Review Integrating Three Decades of Multidisciplinary Research. *Sleep Med Rev* **2020**, *50*, 101250. doi: 10.1016/j.smrv.2019.101250
11. Torelli, F.; Moscufo, N.; Garreffa, G.; Placidi, F.; Romigi, A.; Zannino, S.; Bozzali, M.; Fasano, F.; Giulietti, G.; Djonlagic, I.; et al. Cognitive Profile and Brain Morphological Changes in Obstructive Sleep Apnea. *Neuroimage* **2011**, *54*, 787–793. doi: 10.1016/j.neuroimage.2010.09.065
12. Arias-Cavieres, A.; Fonteh, A.; Castro-Rivera, C.I.; Garcia, A.J. Intermittent Hypoxia Causes Targeted Disruption to NMDA Receptor Dependent Synaptic Plasticity in Area CA1 of the Hippocampus. *Exp Neurol* **2021**, *344*, 113808. doi: 10.1016/j.expneurol.2021.113808
13. Zhang, K.; Ma, D.; Wu, Y.; Xu, Z. Impact of Chronic Intermittent Hypoxia on Cognitive Function and Hippocampal Neurons in Mice: A Study of Inflammatory and Oxidative Stress Pathways. *Nat Sci Sleep* **2024**, *16*, 2029–2043. doi: 10.2147/NSS.S489232

 doi:10.20944/preprints202506.2250.v1

14. Li, F.; Li, D.; Gong, B.; Song, Z.; Yu, Y.; Yu, Y.; Yang, Y. Sevoflurane Aggravates Cognitive Impairment in OSAS Mice through Tau Phosphorylation and Mitochondrial Dysfunction. *Exp Neurol* **2025**, *384*, 115056. doi: 10.1016/j.expneurol.2024.115056
15. Zhao, Y.; Yang, S.; Guo, Q.; Guo, Y.; Zheng, Y.; Ji, E. Shashen-Maidong Decoction Improved Chronic Intermittent Hypoxia-Induced Cognitive Impairment through Regulating Glutamatergic Signaling Pathway. *J Ethnopharmacol* **2021**, *274*, 114040. doi: 10.1016/j.jep.2021.114040
16. Aubrecht, T.G.; Weil, Z.M.; Magalang, U.J.; Nelson, R.J. Dim Light at Night Interacts with Intermittent Hypoxia to Alter Cognitive and Affective Responses. *Am J Physiol Regul Integr Comp Physiol* **2013**, *305*, 78–86. doi: 10.1152/ajpregu.00100.2013
17. Lavie, L. Oxidative Stress in Obstructive Sleep Apnea and Intermittent Hypoxia - Revisited - The Bad Ugly and Good: Implications to the Heart and Brain. *Sleep Med Rev* **2015**, *20*, 27–45. doi: 10.1016/j.smrv.2014.07.003
18. Dewan, N.A.; Nieto, F.J.; Somers, V.K. Intermittent Hypoxemia and OSA: Implications for Comorbidities. *Chest* **2015**, *147*, 266–274. doi: 10.1378/chest.14-0500
19. Xu, L.; Yang, Y.; Chen, J. The Role of Reactive Oxygen Species in Cognitive Impairment Associated with Sleep Apnea. *Exp Ther Med* **2020**, *20*, 4. doi: 10.3892/etm.2020.9132
20. Zhou, W.; Feng, X.; Li, H.; Wang, L.; Zhu, B.; Liu, W.; Zhao, M.; Yao, K.; Ren, C. Inactivation of LARS2, Located at the Commonly Deleted Region 3p21.3, by Both Epigenetic and Genetic Mechanisms in Nasopharyngeal Carcinoma. *Acta Biochim Biophys Sin (Shanghai)* **2009**, *41*, 54–62. doi: 10.1093/abbs/gmn006
21. Neyroud, A.S.; Rudinger-Thirion, J.; Frugier, M.; Riley, L.G.; Bidet, M.; Akloul, L.; Simpson, A.; Gilot, D.; Christodoulou, J.; Ravel, C.; et al. LARS2 Variants Can Present as Premature Ovarian Insufficiency in the Absence of Overt Hearing Loss. *European Journal of Human Genetics* **2023**, *31*, 453–460. doi: 10.1038/s41431-022-01252-1
22. Kiss, H.; Kedra, D.; Yang, Y.; Kost-Alimova, M.; Kiss, C.; O'Brien, K.P.; Fransson, I.; Klein, G.; Imreh, S.; Dumanski, J.P. A Novel Gene Containing LIM Domains (LIMD1) Is Located within the Common Eliminated Region 1 (C3CER1) in 3p21.3. *Hum Genet* **1999**, *105*, 552–559. doi: 10.1007/s004399900188
23. Chen, J.; Liu, W. Lin28a Induced Mitochondrial Dysfunction in Human Granulosa Cells via Suppressing LARS2 Expression. *Cell Signal* **2023**, *103*, 110536. doi: 10.1016/j.cellsig.2022.110536
24. Qian, W.; Yuan, L.; Zhuge, W.; Gu, L.; Chen, Y.; Zhuge, Q.; Ni, H.; Lv, X. Regulating Lars2 in Mitochondria: A Potential Alzheimer's Therapy by Inhibiting Tau Phosphorylation. *Neurotherapeutics* **2024**, *21*, e00353. doi: 10.1016/j.neurot.2024.e00353
25. Feng, S.; Wan, S.; Liu, S.; Wang, W.; Tang, M.; Bai, L.; Zhu, Y. LARS2 Regulates Apoptosis via ROS-Mediated Mitochondrial Dysfunction and Endoplasmic Reticulum Stress in Ovarian Granulosa Cells. *Oxid Med Cell Longev* **2022**, *2022*, 5501346. doi: 10.1155/2022/5501346
26. Vogel, B.E.; Hedgecock, E.M. Hemicentin, a Conserved Extracellular Member of the Immunoglobulin Superfamily, Organizes Epithelial and Other Cell Attachments into Oriented Line-Shaped Junctions. *Development* **2001**, *128*, 883–894. doi: 10.1242/dev.128.6.883
27. Gao, H.; Tao, Y.; He, Q.; Song, F.; Saffen, D. Functional Enrichment Analysis of Three Alzheimer's Disease Genome-Wide Association Studies Identities DAB1 as a Novel Candidate Liability/Protective Gene. *Biochem Biophys Res Commun* **2015**, *463*, 490–495. doi: 10.1016/j.bbrc.2015.05.044
28. Yang, J.; Lu, X.; Hao, J.L.; Li, L.; Ruan, Y.T.; An, X.N.; Huang, Q.L.; Dong, X.M.; Gao, P. VSTM2L Protects Prostate Cancer Cells against Ferroptosis via Inhibiting VDAC1 Oligomerization and Maintaining Mitochondria Homeostasis. *Nat Commun* **2025**, *16*, 1160. doi: 10.1038/s41467-025-56494-6
29. Török, I.; Herrmann-Horle, D.; Kiss, I.; Tick, G.; Speer, G.; Schmitt, R.; Mechler, B.M. Down-Regulation of RpS21, a Putative Translation Initiation Factor Interacting with P40, Produces Viable Minute Imagos and Larval Lethality with Overgrown Hematopoietic Organs and Imaginal Discs. *Mol Cell Biol* **1999**, *19*, 2308–2321. doi: 10.1128/MCB.19.3.2308
30. Ahmed, S.M.U.; Luo, L.; Namani, A.; Wang, X.J.; Tang, X. Nrf2 Signaling Pathway: Pivotal Roles in Inflammation. *Biochim Biophys Acta Mol Basis Dis* **2017**, *1863*, 585–597. doi: 10.1016/j.bbadis.2016.11.005

 doi:10.20944/preprints202506.2250.v1

31. Holmström, K.M.; Baird, L.; Zhang, Y.; Hargreaves, I.; Chalasani, A.; Land, J.M.; Stanyer, L.; Yamamoto, M.; Dinkova-Kostova, A.T.; Abramov, A.Y. Nrf2 Impacts Cellular Bioenergetics by Controlling Substrate Availability for Mitochondrial Respiration. *Biol Open* **2013**, *2*, 761–770. doi: 10.1242/bio.20134853
32. Niture, S.K.; Jaiswal, A.K. Nrf2 Protein Up-Regulates Antiapoptotic Protein Bcl-2 and Prevents Cellular Apoptosis. *Journal of Biological Chemistry* **2012**, *287*, 9873–9886. doi: 10.1074/jbc.M111.312694
33. Zhang, M.; An, C.; Gao, Y.; Leak, R.K.; Chen, J.; Zhang, F. Emerging Roles of Nrf2 and Phase II Antioxidant Enzymes in Neuroprotection. *Prog Neurobiol* **2013**, *100*, 30–47. doi: 10.1016/j.pneurobio.2012.09.003
34. Kim, S.M.; Kim, H.; Lee, J.S.; Park, K.S.; Jeon, G.S.; Shon, J.; Ahn, S.W.; Kim, S.H.; Lee, K.M.; Sung, J.J.; et al. Intermittent Hypoxia Can Aggravate Motor Neuronal Loss and Cognitive Dysfunction in ALS Mice. *PLoS One* **2013**, *8*, e81808. doi: 10.1371/journal.pone.0081808
35. Kim, S.K.; Kwon, D.A.; Kim, Y.S.; Lee, H.S.; Kim, H.K.; Kim, W.K. Standardized Extract (HemoHIM) Protects against Scopolamine-Induced Amnesia in a Murine Model. *Evidence-based Complementary and Alternative Medicine* **2021**, *2021*, 8884243. doi: 10.1155/2021/8884243
36. Zhou, Y.; Zhou, B.; Pache, L.; Chang, M.; Khodabakhshi, A.H.; Tanaseichuk, O.; Benner, C.; Chanda, S.K. Metascape Provides a Biologist-Oriented Resource for the Analysis of Systems-Level Datasets. *Nat Commun* **2019**, *10*, 1523. doi: 10.1038/s41467-019-09234-6
37. Evans, A.K.; Park, H.H.; Woods, C.E.; Lam, R.K.; Rijsketic, D.R.; Xu, C.; Chu, E.K.; Ciari, P.; Blumenfeld, S.; Vidano, L.M.; et al. Impact of Noradrenergic Inhibition on Neuroinflammation and Pathophysiology in Mouse Models of Alzheimer's Disease. *J Neuroinflammation* **2024**, *21*, 322. doi: 10.1186/s12974-024-03306-1
38. Salih, D.A.M.; Rashid, A.J.; Colas, D.; de la Torre-Ubieta, L.; Zhu, R.P.; Morgan, A.A.; Santo, E.E.; Ucar, D.; Devarajan, K.; Cole, C.J.; et al. FoxO6 Regulates Memory Consolidation and Synaptic Function. *Genes Dev* **2012**, *26*, 2780–2801. doi: 10.1101/gad.208926.112
39. Wang, X.; Xie, Y.; Fan, X.; Wu, X.; Wang, D.; Zhu, L. Intermittent Hypoxia Training Enhances Aβ Endocytosis by Plaque Associated Microglia via VPS35-Dependent TREM2 Recycling in Murine Alzheimer's Disease. *Alzheimer's Research and Therapy* **2024**, *16*, 121. doi: 10.1186/s13195-024-01489-6
40. Yang, X.; Chang, L.; Liu, Z.; Geng, X.; Wang, R.; Yin, X.; Fan, W.; Zhao, B.Q. Neddylation in the Chronically Hypoperfused Corpus Callosum: MLN4924 Reduces Blood-Brain Barrier Injury via ERK5/KLF2 Signaling. *Exp Neurol* **2024**, *371*, 114587. doi: 10.1016/j.expneurol.2023.114587
41. Song, J.; Wang, T.; Hong, J.S.; Wang, Y.; Feng, J. TFEB-Dependent Autophagy-Lysosomal Pathway Is Required for NRF2-Driven Antioxidative Action in Obstructive Sleep Apnea-Induced Neuronal Injury. *Cell Signal* **2025**, *128*, 111630. doi: 10.1016/j.cellsig.2025.111630
42. Yao, Q.; Long, C.; Yi, P.; Zhang, G.; Wan, W.; Rao, X.; Ying, J.; Liang, W.; Hua, F. C/EBPβ: A Transcription Factor Associated with the Irreversible Progression of Alzheimer's Disease. *CNS Neurosci Ther* **2024**, *30*, e14721. doi: 10.1111/cns.14721
43. Gokce, M.; Velioglu, H.A.; Bektay, M.Y.; Guler, E.M. Evaluating the Clinical Significance of Diazepam Binding Inhibitor in Alzheimer's Disease: A Comparison with Inflammatory, Oxidative, and Neurodegenerative Biomarkers. *Gerontology* **2023**, *69*, 1104–1112. doi: 10.1159/000531849
44. Wang, F.; Han, X.; Mu, Q.; Chen, H.; Wu, Y.; Kang, Y.; Liu, Y. Cerebrospinal Fluid Mesencephalic Astrocyte-Derived Neurotrophic Factor: A Moderating Effect on Sleep Time and Cognitive Function. *J Psychiatr Res* **2024**, *176*, 33–39. doi: 10.1016/j.jpsychires.2024.05.048
45. Xie, R.; Wang, Z.; Liu, T.; Xiao, R.; Lv, K.; Wu, C.; Luo, Y.; Cai, Y.; Fan, X. AAV Delivery of ShRNA Against TRPC6 in Mouse Hippocampus Impairs Cognitive Function. *Front Cell Dev Biol* **2021**, *9*, 688655. doi: 10.3389/fcell.2021.688655